Inorganica Chimica Acta 362 (2009) 1553–1558

Contents lists available at ScienceDirect

Inorganica Chimica Acta

journal homepage: www.elsevier.com/locate/ica

A study of the second coordination sphere in 8-azaxanthinato salts of divalent metal aquacomplexes

Carmen R. Maldonado, Miguel Quirós *, Juan M. Salas, Antonio Rodríguez-Diéguez

Departamento de Química Inorgánica, Facultad de Ciencias, Universidad de Granada, 18071 Granada, Spain

ARTICLE INFO

Article history:
Received 20 May 2008
Received in revised form 16 July 2008
Accepted 24 July 2008
Available online 5 August 2008

Keywords:
Azapurines
Azaxanthines
Triazolopyrimidines
Hydrogen bonds
Second coordination sphere

ABSTRACT

The interaction of the 4,6-dimethyl and 4-monomethyl derivatives of 1,2,3-triazolo[4,5-*d*]pyrimidin-5,7-dione (which may be named also as purine derivatives, 1,3-dimethyl-8-azaxanthine, Hdmax and 3-methyl-8-azaxanthine, H3max) with the divalent cations of Mn, Co, Ni, Zn and Cd in aqueous media generate solids with formulation $ML_2 \cdot 6H_2O$. The crystal structure of the Mn and Cd compounds with dmax and the Cd compound with 3max have been determined by single-crystal X-ray diffraction revealing that the compounds are salts with $[M(H_2O)_6]^{2+}$ as cations and $dmax^-$ or $3dmax^-$ as anions. The second-sphere interactions in these compounds have been analysed, consisting in a network of very well-defined hydrogen bonds, with all available potential donor and acceptor positions involved. The topology of the motifs generated by these hydrogen bonds has been characterised, adapting to the second coordination sphere concepts usually applied to the first (chelate, bridge, monodentate, ...). Monodimensional (tapes) superstructures with the building blocks rather tightly bounded appear in the compounds with $dmax^-$ as anion, whereas the corresponding superstructure in the Cd compound with $3max^-$ is bidimensional. These superstructures further interact among them in a less tight fashion to generate the three dimensional crystal structures. Powder X-ray diffraction strongly suggests that Mn, Co, Zn and Cd compounds of each ligand are isostructural, so the results of the samples determined by single-crystal X-ray diffraction may be extended to all these compounds. On the other hand, powder X-ray diffraction indicates that the nickel compounds have a different structure and the spectroscopic data for these compounds suggest that the ligand is directly attached to the metal for them.

1. Introduction

The study of the interaction of metal ions with nucleic acids, their constituents and their analogues has been a largely developed research topic in the last decades. These interactions have important biochemical implications in nucleotide biochemistry, genetic information storage and transfer, and control of gene expression [1]. The main interest of these studies uses to be the direct bonds formed between cation and ligand, the so called first coordination sphere, relegating the weakest interactions known as second coordination sphere to a secondary role. Nevertheless, these interactions are, in discrete compounds, the responsible for building the crystalline structures.

Among these interactions, hydrogen bonding is probably the most important one in many systems. Hydrogen bonds, when acting together, become much stronger since they lean on each other, phenomenon called cooperativity in scientific terms (1+1 > 2) [2]. Currently, the hydrogen bond is more than ever a topic of vital scientific research because it plays a key role in a vast number of chemical systems, which range from inorganic to biological chemistry [3]. One of the most clear examples of this is the molecular recognition between the complementary bases in DNA, responsible of the formation of the well-known double helix. Thus, hydrogen bonding could, in principle, be used as the way of joining the building blocks in the rational design of supramolecular structures [4]; however, performing this crystal engineering task in a accurately predictable manner using synthons with several different possible donors and acceptors groups cannot be easily done.

In the search for new compounds as effective antiviral and antitumour therapy, the synthesis of many modified nucleobases has been reported. For example, replacement of the imidazole ring in purines for 1,2,3-triazole to build 8-azapurines (1,2,3-triazolo-[4,5-*d*]pyrimidines) [5–7] leads to significant changes in the chemical and biological properties such as their activity as anti-tumour drugs [8,9]. Scheme 1 compares these two bicyclic systems, depicting the IUPAC numbering scheme used for the triazolopyrimidine derivatives and the biochemical numbering scheme, more usual when dealing with purines. IUPAC numbering scheme is used throughout this article, though the terms “8-azapurine” or “8-azaxanthine”, etc. are still used since they are more compact than the proper IUPAC name of the compounds.

---

* Corresponding author. Tel.: +34 958240441; fax: +34 958248526.
E-mail address: mquiros@ugr.es (M. Quirós).

0020-1693/$ - see front matter © 2008 Elsevier B.V. All rights reserved.
doi:10.1016/j.ica.2008.07.029

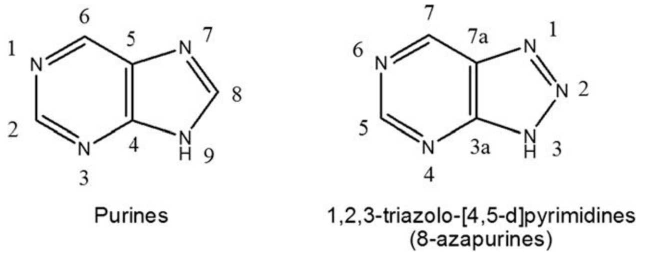

Scheme 1.

The interaction of transition metal ions with 8-azapurine derivatives (8-azaadenines, 8-azaguanines, 8-azaxanthines, 8-azahypoxanthines, etc.) has been the subject of relatively few chemical, spectroscopic and crystallographic studies. The small amount of accumulated data indicate that these interactions are quite different to the interactions with purines [10–24]. The only previous example of a crystal structure of a metal complex containing an 8-azaxanthine derivative was reported by our research group in the eighties [17].

Following this research line, we have studied the interaction in aqueous medium of a series of divalent metal ions (Mn, Co, Ni, Zn and Cd) with the anionic form of two 8-azaxanthines: 1,3-dimethyl-8-azaxanthine (Hdmax) and 3-methyl-8-azaxanthine (H3max). The systematic IUPAC names of these compounds are 4,6-dimethyl-1,2,3-triazolo[4,5-*d*]pyrimidin-5,7-dione and 4-methyl-1,2,3-triazolo[4,5-*d*]pyrimidin-5,7(6*H*)-dione, respectively. The spectroscopic and X-ray diffraction data studies of the isolated solids reveal that they are, with the possible exception of the Ni compounds, ionic salts of the corresponding hexaacuacomplexes with the organic moieties as counteranions without a direct bond between the metal and the azaxanthine derivative. Nevertheless, these compounds exhibit an interesting and very well-defined network of hydrogen bonds, with all potential acceptor and donor sites involved, which build their three-dimensional architectures, this second coordination sphere being the main subject of the present study. Less extensive H-bond networks have been previously observed in azapurine metal compounds for bis(8-azahypoxanthinato)tetraaquacadmium(II) [12] and tetraaquabis(8-azahypoxanthinato)mercury(II) [14] but have not been studied in detail.

2. Experimental

2.1. Synthesis of the compounds

The synthesis of ligands 1,3-dimethyl-8-azaxanthine (Hdmax) and 3-methyl-8-azaxanthine (H3max) was carried out according to the published method of Nübel & Pfleiderer [25]. Other reagents were obtained from commercial sources and used without further purification.

4,6-Dimethyl-1,2,3-triazolo[4,5-*d*]pyrimidin-5,7-dione (1,3-dimethyl-8-azaxanthine, Hdmax). ^{1}H NMR (300.20 MHz, DMSO-d_6): δ 3.23 (s, 3H, *H*41/*H*42/*H*43), δ 3.42 (s, 3H, *H*61/*H*62/*H*63). ^{13}C NMR (75.49 MHz, DMSO-d_6): δ 27.9 (CH_3, *C*4), δ 30.6 (CH_3, *C*6), δ 123.5 (C, *C*7a), δ 148.5 (C, *C*3a), δ 150.8 (C, *C*5), δ 155.9 (C, *C*7).

4-Methyl-1,2,3-triazolo[4,5-*d*]pyrimidin-5,7(6*H*)-dione (3-methyl-8-azaxanthine, H3max). ^{1}H NMR (300.20 MHz, DMSO-d_6): δ 3.37 (s, 3H, *H*41/ *H*42/*H*43), δ 11.41 (s, 1H, *H*6). ^{13}C NMR (75.49 MHz, DMSO-d_6): δ 29.6 (CH_3, *C*4), δ 124.2 (C, *C*7a), δ 150.3 (C, *C*3a), δ 150.8 (C, *C*5), δ 156.3 (C, *C*7).

The sodium salts of these compounds were obtained by mixing aqueous solutions of each of them (1 mmol, 30 mL) with NaOH solutions (1.5 mmol, 5 mL). Elemental analysis data reveal that the salts crystallize as hydrates.

Na(dmax) · 2.5H_2O, white powder. *Anal.* Calc. for $C_6H_{11}NaN_5O_{4.5}$: C, 29.0; H, 4.5; N, 28.2. Found: C, 28.8; H, 4.1; N, 28.4%. ^{1}H NMR (300.20 MHz, DMSO-d_6): δ 3.21 (s, 3H, H41/H42/H43), δ 3.44 (s, 3H, H61/H62/H63). ^{13}C NMR (75.49 MHz, DMSO-d_6): δ 27.4 (CH_3, C4), δ 30.5 (CH_3, C6), δ 122.2 (C, C7a), δ 149.9 (C, C3a), δ 151.4 (C, C5), δ 157.1 (C, C7).

Na(3max) · 2.5H_2O, white powder. *Anal.* Calc. for $C_5H_9NaN_5O_{4.5}$: C, 25.6; H, 3.9; N, 29.9. Found: C, 25.4; H, 3.3; N, 29.7%. ^{1}H NMR (300.20 MHz, DMSO-d_6): δ 3.37 (s, 3H, *H*41/*H*42/*H*43), δ 10.33 (bs, H, *H*6). ^{13}C NMR (75.49 MHz, DMSO-d_6): δ 29.6 (CH_3, *C*4), δ 122.9 (C, *C*7a), δ 151.7 (C, *C*3a), δ 152.0 (C, *C*5), δ 157.6 (C, *C*7).

Aquacomplexes salts were obtained by mixing two aqueous solutions, 15 mL each, one containing 2 mmol of the sodium salt of the appropriate ligand and the other containing 1 mmol of the metal salt (sulphate for Mn and nitrate for Co, Ni, Zn and Cd). From the solutions containing Na(dmax) and manganese sulphate, Na(dmax) and cadmium nitrate and Na(3max) and cadmium nitrate, colourless crystals suitable for X-ray studies were isolated. The other complexes were obtained as powders from their corresponding solutions after several hours. In all cases, the solids were washed with water and ethanol and dried with ether.

From elemental analyses, the following formulae were deduced for the isolated compounds:

[Mn(H_2O)$_6$](dmax)$_2$ (**1**), colourless crystals. *Anal.* Calc. for $C_{12}H_{24}MnN_{10}O_{10}$: C, 27.5; H, 4.6; N, 26.8. Found: C, 27.8; H, 4.8; N, 26.8%.

[Co(H_2O)$_6$](dmax)$_2$ (**2**), pale pink microcrystalline powder. *Anal.* Calc. for $C_{12}H_{24}CoN_{10}O_{10}$: C, 27.3; H, 4.6; N, 26.6. Found: C, 27.8; H, 4.7; N, 26.5%.

Ni(dmax)$_2$ · 6H_2O (**3**), pale blue powder. *Anal.* Calc. for $C_{12}H_{24}N_{10}NiO_{10}$: C, 27.3; H, 4.6; N, 26.6. Found: C, 26.8; H, 4.5; N, 26.3%.

[Zn(H_2O)$_6$](dmax)$_2$ (**4**), pale yellow microcrystalline powder. *Anal.* Calc. for $C_{12}H_{24}N_{10}O_{10}Zn$: C, 27.0; H, 4.5; N, 26.2. Found: C, 26.5; H, 4.4; N, 25.8%. ^{1}H NMR (300.20 MHz, DMSO-d_6): δ 3.23 (s, 3H, *H*41/*H*42/*H*43), δ 3.47 (s, 3H, *H*61/*H*62/*H*63). ^{13}C NMR (75.49 MHz, DMSO-d_6): δ 27.8 (CH_3, *C*4), δ 30.7 (CH_3, *C*6), δ 123.4 (C, *C*7a), δ 149.6 (C, *C*3a), δ 151.2 (C, *C*5), δ 156.6 (C, *C*7).

[Cd(H_2O)$_6$](dmax)$_2$ (**5**), colourless crystals. *Anal.* Calc. for $C_{12}H_{24}CdN_{10}O_{10}$: C, 24.8; H, 4.2; N, 24.1. Found: C, 25.0; H, 4.4; N, 24.3%. ^{1}H NMR (300.20 MHz, DMSO-d_6): δ 3.23 (s, 3H, *H*41/ *H*42/*H*43), δ 3.46 (s, 3H, *H*61/*H*62/*H*63). ^{13}C NMR (75.49 MHz, DMSO-d_6): δ 27.6 (CH_3, *C*4), δ 30.6 (CH_3, *C*6), δ 122.8 (C, *C*7a), δ 149.7 (C, *C*3a), δ 151.3 (C, *C*5), δ 156.9 (C, *C*7).

[Mn(H_2O)$_6$](3max)$_2$ (**6**), pale yellow microcystalline powder. *Anal.* Calc. for $C_{10}H_{20}MnN_{10}O_{10}$: C, 24.3; H, 4.1; N, 28.3. Found: C, 24.1; H, 4.6; N, 28.2%.

[Co(H_2O)$_6$](3max)$_2$ (**7**), pale orange microcrystalline powder. *Anal.* Calc. for $C_{10}H_{20}CoN_{10}O_{10}$: C, 24.1; H, 4.0; N, 28.1. Found: C, 23.8; H, 4.2; N, 27.5%.

Ni(3max)$_2$ · 6.5H_2O (**8**), mauve powder. *Anal.* Calc. for $C_{10}H_{21}N_{10}NiO_{10.5}$: C, 23.6; H, 4.2; N, 27.6. Found: C, 24.0; H, 4.5; N, 27.2%.

[Zn(H_2O)$_6$](3max)$_2$ (**9**), pale yellow microcrystalline powder. *Anal.* Calc. for $C_{10}H_{20}N_{10}O_{10}Zn$: C, 23.8; H, 4.0; N, 27.7. Found: C, 23.8; H, 4.0; N, 27.2%. ^{1}H NMR (300.20 MHz, DMSO-d_6): δ 3.40 (s, 3H, *H*41/*H*42/*H*43), δ 10.95 (s, H, *H*6). ^{13}C NMR (75.49 MHz, DMSO-d_6): δ 29.7 (CH_3, *C*4), δ 124.1 (C, *C*7a), δ 151.2 (C, *C*3a), δ 151.4 (C, *C*5), δ 156.9 (C, *C*7).

[Cd(H_2O)$_6$](3max)$_2$ (**10**), colourless crystals. *Anal.* Calc. for $C_{10}H_{20}CdN_{10}O_{10}$: C, 21.7; H, 3.6; N, 25.3. Found: C, 22.0; H, 3.9; N, 25.3%. ^{1}H NMR (300.20 MHz, DMSO-d_6): δ 3.39 (s, 3H, *H*41/ *H*42/*H*43), δ 10.68 (s, H, *H*6). ^{13}C NMR (75.49 MHz, DMSO-d_6): δ 29.6 (CH_3, *C*4), δ 123.4 (C, *C*7a), δ 151.3 (C, *C*3a), δ 151.5 (C, *C*5), δ 157.3 (C, *C*7).

2.2. Instrumentation

Microanalysis of C, H and N were performed in a Fisons Instruments EA-1008 analyser. Thermal behaviour was studied under an air flow in Shimadzu TGA-50 and Shimadzu DSC-50 equipment, at heating rates of 20 °C min^{-1} and 10 °C min^{-1}, respectively. Reflectance diffuse spectra were made on a VARIAN model CARY-5E spectrophotometer. NMR spectra were recorded in D_6[dmso] on Varian Inova 300 MHz instrument, solvent signals (^{1}H, ^{13}C) were used as internal references (all this equipment is sited at the Centre of Scientific Instrumentation of the University of Granada). IR spectra were recorded on a ThermoNicolet IR 200 spectrometer using KBr pellets.

2.3. Crystallography

Data were collected, at room temperature for **1** and **10** and at 100 K for **5**, in a Bruker SMART APEX CCD system with Mo *K*α radiation ($\lambda = 0.7107$ Å). Data were corrected for absorption (multi-scan, transmission ranges, 0.904–0.780, 0.967–0.814 and 0.954–0.807 for **1**, **5** and **10**, respectively). The structures were solved by the heavy atom method and anisotropically refined in F^2 using SHELXL-97 [26]. Hydrogen atoms of the heterocycles were placed in ideal positions whereas those of water molecules were clearly spotted in the ΔF maps and refined with restrained O–H distance (0.85(1) Å). Isotropic thermal parameters of all H atoms fixed to 1.2 times the equivalent isotropic thermal parameter of their parent atoms. Table 1 summarizes the crystallographic data for these compounds.

Powder X-ray diffraction data have been collected on a θ:θ Bruker AXS D8 vertical scan diffractometer with Cu Kα radiation ($\lambda = 1.5418$ Å). The powders were gently ground in an agate mortar and then deposited with care in the hollow of an aluminium holder equipped with a zero background plate. Le Bail fits of the diffractograms acquired were performed with the aid of TOPAS [27].

Table 1
Crystal data

Compound	**1**	**5**	**10**
Chemical formula	$C_{12}H_{24}MnN_{10}O_{10}$	$C_{12}H_{24}CdN_{10}O_{10}$	$C_{10}H_{20}CdN_{10}O_{10}$
Formula weight	523.35	580.81	552.76
Crystal size (mm)	0.47 × 0.34 × 0.15	0.38 × 0.26 × 0.03	0.37 × 0.07 × 0.04
Crystal system	triclinic	triclinic	triclinic
Space group	$P\bar{1}$	$P\bar{1}$	$P\bar{1}$
Unit cell dimensions			
a (Å)	7.7462(14)	7.7334(5)	6.8110(8)
b (Å)	8.0979(15)	7.8437(5)	8.7316(10)
c (Å)	9.9361(18)	9.9055(6)	8.9234(10)
α (°)	74.563(3)	75.722(1)	86.413(2)
β (°)	80.102(3)	80.977(1)	67.813(2)
γ (°)	63.533(3)	65.012(1)	87.315(2)
Volume (Å^3)	536.79(17)	526.84(6)	490.27(10)
Z	1	1	1
D_{calc} (calculated, g/cm^3)	1.619	1.831	1.872
Absorption coefficient (mm^{-1})	0.688	1.111	1.189
θ Range for data collection (°)	2.13–28.27	2.13–28.26	2.34–28.40
Reflections collected/unique	6253/2425	6126/2384	5761/2223
Data/restrains/parameters	2425/6/171	2384/6/171	2223/6/161
Goodness-of-fit on F^2	1.031	1.087	1.042
R ($I \geqslant 2\,\sigma(I)$)	0.0372	0.0242	0.0250
wR^2 (all data)	0.1126	0.0624	0.0640
Largest difference peak and hole (e Å^{-3})	0.309 and −0.326	0.754 and −0.512	0.443 and −0.304

3. Results and discussion

3.1. X-ray structural studies: the building blocks

Three of the isolated compounds (**1**, **5** and **10**) have been obtained as crystals suitable for monocrystal X-ray analysis and their crystal structures have been determined. The three compounds are ionic salts with $[M(H_2O)_6]^{2+}$ as the cation (M = Mn for **1** and M = Cd for **5** and **10**) and the deprotonated form of the 8-azaxanthine derivative as counteranion (dmax$^-$ for **1** and **5** and 3max$^-$ for **10**). Fig. 1 displays a view of the basic ionic units in **5**, those in the other two compounds are very similar. The metal atoms lie in crystallographic inversion centres and the respective octahedra are appreciably distorted, surely due to the hydrogen bonding interactions, this distortion being higher for the compounds with dmax, metal–water distances ranging from 2.1413(15) to 2.1983(16) Å and from 2.2472(14) to 2.2974(15) Å for **1** and **5**, respectively, whereas the maximum deviations from perpendicularity of cis bond angles are 2.01° and 2.68°, respectively. The octahedron in **10** is somewhat more regular with distances in the 2.2545(18)–2.2658(18) Å range and deviations from perpendicularity below 1.2°. The ionization of the acidic protons of Hdmax and 3Hmax, located at the nitrogen atom at position 2 in the crystal structures of the free ligands [6],[17], leads to a ~5° closing of the endocyclic angle at that atom and the opening of the adjacent endocyclic angles.

Nevertheless, the main interest of these structures does not lie in the first coordination sphere but in the second, which generates a three-dimensional hydrogen bonded network, with all potential donor and acceptor sites involved. The networks are quite well characterized, since all hydrogen atoms have been clearly spotted in the crystallographic analysis. The structures are a good example of how concepts usually applied to the first coordination sphere find clear analogies in the second coordination sphere, so we may use terms like "monodentate", "bridging ligand", "chelate" and so on. The results for the isostructural compounds **1** and **5** are presented firstly and those of compound **10** are described afterwards. Table 2 lists hydrogen bond parameters for the three compounds.

3.2. Hydrogen bonding network in compounds 1 and 5

Compounds **1** and **5** are isostructural and therefore the topology of the hydrogen bonding network is identical for both. The ligand has five potential hydrogen acceptor sites (N1, N2, N3, O5 and O7), while the water molecules provide twelve donor sites for the cation, all of these sites are involved in hydrogen bonding building the supramolecular structure of these compounds. Therefore, the second coordination sphere number of the metal is twelve (twelve atoms from eight anions) and that of the anion is six (O5 accepting two H-bonds).

N2 and N3 interact with water molecules belonging to the same hexaaquacation, this closes a seven-atom ring (the metal, two oxygens, two hydrogens and two nitrogens) that may be defined as a "chelate", this pattern may be represented in a condensed way as $R_2^2(7)$ according to the graph set notation proposed by Etter, Bernstein et al. [28,29]: R indicates a ring, the degree (in parentheses) is the number of atoms in the ring, and the super- and subscripts represent the number of hydrogen bond acceptors and donors in the motif, respectively. N1 and O7 define another chelate (in this case $R_2^2(9)$) with another $[M(H_2O)_6]^{2+}$ cation. These chelating interactions build tape structures that grow in the (1, −1, 0) direction (Fig. 2); a tape is defined as an infinite monodimensional

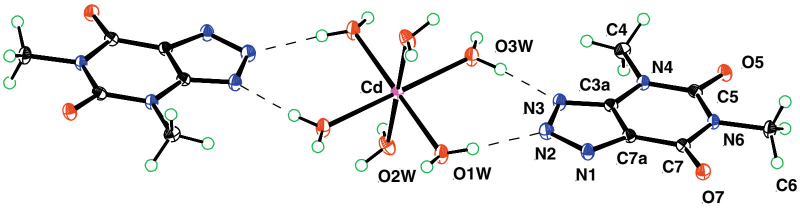

Fig. 1. View of the basic ionic unit of compound **5**.

Table 2
Hydrogen-bond geometry (Å, °)

	Compound **1**		Compound **5**	
	d(D···A)	∠(DHA)	*d*(D···A)	∠(DHA)
O(1W)–H(11W)···N(2)	2.799(2)	167(3)	2.792(2)	162(3)
O(1W)–H(12W)···N(1)#2	2.789(2)	172(3)	2.783(2)	172(3)
O(2W)–H(21W)···O(5)#3	2.779(2)	164(3)	2.757(2)	168(3)
O(2W)–H(22W)···O(5)#4	2.855(2)	168(3)	2.839(2)	171(3)
O(3W)–H(31W)···N(3)	2.756(2)	172(3)	2.744(2)	174(3)
O(3W)–H(32W)···O(7)#5	2.7998(19)	161(3)	2.771(2)	161(3)

Symmetry transformations used to generate equivalent atoms: #2 $-x+2, -y, -z+1$; #3 $x-1, y, z+1$; #4 $-x+1, -y+1, -z$; #5 $x-1, y+1, z$

	Compound **10** *d*(D···A)	∠(DHA)
O(1W)–H(12W)···N(1)	2.758(2)	168(3)
O(1W)–H(11W)···O(7)#2	2.783(2)	163(3)
O(2W)–H(21W)···O(5)#3	2.778(2)	173(3)
O(2W)–H(22W)···O(7)#4	2.817(2)	162(3)
O(3W)–H(32W)···N(2)	2.845(2)	156(3)
O(3W)–H(31W)···N(3)#5	2.831(3)	174(3)
N(6)–H(6)···O(5)#6	2.896(2)	168.9

Symmetry transformation used to generate equivalent atoms: #2 $-x+1, -y+1, -z$ #3 $x-1, y+1, z+1$; #4 $x-1, y, z+1$; #5 $-x+1, -y, -z+1$; #6 $-x+2, -y, -z-1$

structure in which the components are linked by more than one hydrogen bond, with the hydrogen bonds approximately coplanar [4]. A third ring motif $R^4_4(10)$ involving two cations and two anions appears in the tape around crystallographic inversion centres. The anion is roughly coplanar with the tape.

The tapes are linked by the monodentate interactions between the "out-of-tape" water molecule (O2W) and the O5 atom of neighbouring tapes, thus generating the three-dimensional network. This interaction between two neighbouring O2W water molecules and two O5 carbonyl oxygens defines another centrosymmetric ring (O_4H_4, $R^2_4(8)$). Apart from H-bonding, another interaction that links tapes is the stacking between pairs of anions, the two components of the couple are related by an inversion centre and dispose parallel to each other, with the imidazole ring of one of the anions over the pyrimidine ring of the other and separated 3.31 Å.

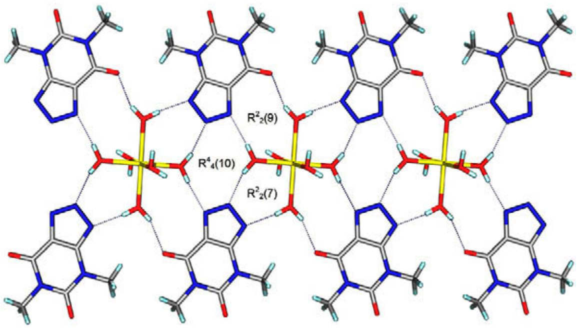

Fig. 2. Tape along the (1, −1, 0) direction built by the hydrogen bond interactions in compound **5**.

3.3. Hydrogen bonding network in compound ***10***

The replacement of a methyl group by an hydrogen at position 6 generates a donor site (H6) for the ligand 3max⁻ in addition to the five acceptor sites (N1, N2, N3, O5 and O7) present in dmax⁻, this is the reason why the supramolecular structure in compound **10** is different to the described above for compounds **1** and **5**. The presence of this new donor site makes the anions to associate in pairs due to the hydrogen bonding motif DA–AD (D = N6–H and A = O5, $R^2_2(8)$) across an inversion centre, association of the same kind of that present between guanine and cytosine in DNA structure. An alternative way of describing the structure is to consider that the anionic species in the structure is in fact the couple $(3max)_2{}^{2-}$. This association is also observed between neutral 3max molecules in the crystal structure of the free ligand [17].

The three imidaloze nitrogen atoms accept H-bonds from two cations, N1 and N2 defining a $R^2_2(7)$ "chelate" ring and N2 and N3 forming a centrosymmetric $R^4_4(10)$ motif involving two cations. These interactions lead to the formation of a bidimensional array in the *ab* plane (Fig. 3), with alternating rows of cations and rows of $(3max)_2{}^{2-}$ entities. Additional H-bonds links these layers to each other, the main of which is, possibly the formation of a $R^2_3(10)$ ring involving two water molecules of the same cation, the O5 atom of one of the components of a $(3max)_2{}^{2-}$ entity and the O7 atom of the other, which may be considered also as a chelate if the dimeric entity is considered as if it were an unique ligand. O7 further interacts with another cation, thus acting as a bridge. Alternate sheets

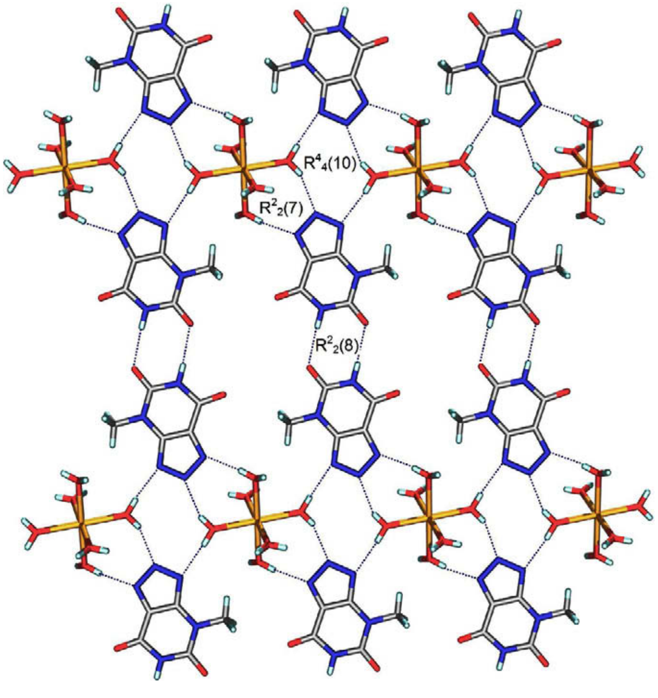

Fig. 3. Layer built by the hydrogen bond interactions in compound **10**.

dispose the rows of cadmium atoms over the rows of middle points of the dimeric anionic units. Stacking along the *c*-axis is observed also between anions of neighbouring sheets (distance, 3.39 Å) but the overlapping between the aromatic rings is worse than in the compounds with dmax.

In resume, these structures are good examples of supramolecular networks whose main glue is hydrogen bonding. H-bonds that assemble cations and anions are very well-defined displaying a great variability in their topology. These compounds are a demonstration of the capability of second-sphere hydrogen bonding as a potential crystal engineering tool for building polymeric metal-containing materials.

3.4. Powder X-ray diffraction analysis

Powder X-ray diffraction diagrams have been recorded for all samples in order to check whether the structural results found for **1**, **5** and **10** may be extended or not to the remaining compounds. Calculated powder diagrams from the single-crystal results have been also performed. A surprising result is found for the cadmium compounds **5** and **10**, the simulated diagram being different to the experimental one: for **5**, there are many additional peaks together with the expected ones whereas for **10**, the experimental pattern is quite different to the calculated. This indicates that a different phase appears in the powder diagrams, partially (**5**) or fully (**10**) replacing the single-crystal phase. It seems that a structure change occurs in the necessary grinding process prior to the recording of the powder diagram, perhaps because of the (partial?) dehydration of the sample. On the other hand, for compound **1**, the simulation reproduces quite faithfully the experimental diagram, indicating that, for this compound, the above described structure survives the grinding process.

The diagrams of the Co and Zn compounds with dmax (**2** and **4**) are very similar to that of **1**, strongly suggesting that the three compounds are isostructural (and also to **5** prior to grinding). Looking at 3max compounds, we find that the diagrams of **6**, **7** and **9** are very similar and also similar to the simulated diagram of **10** (but not to the experimental one), this let us to propose that the Mn, Co and Zn compounds with 3max present the same structure than that of **10** prior to grinding and above described. Le Bail refinements, using the X-ray single-crystal cell parameters of **1** as starting point for dmax compounds and those of **10** for 3dmax compounds, yielded the cell parameters shown in Table 3.

On the other hand, the nickel compounds (**3** and **8**) exhibit powder patterns very different to the other compounds, indicating that they present different crystal structures, this is in agreement with the electronic spectra of these compounds (see below) that point to direct metal coordination to the ligand for nickel.

3.5. Spectral and thermal studies

The 1500–1700 cm^{-1} region of the infrared spectra of the free heterocycles displays three bands (at 1717, 1681 and 1604 cm^{-1} for Hdmax and 1713, 1686 and 1593 cm^{-1} for H3max), assignable to carbonyl stretching and possibly to δ (H_2O), these bands being slightly displaced to lower wavenumbers in the complexes. A new band around 1544 cm^{-1} appears in all compounds with the ligands in anionic form (sodium salts and complexes). An intense characteristic band close to 1310 cm^{-1} is present in all compounds of both ligands in the region expected for vibration modes of the aromatic ring.

Table 3
Unit cell parameters determined from Le Bail refinement of powder data

	a (Å)	*b* (Å)	*c* (Å)	α (°)	β (°)	γ (°)	*V* (Å^3)
1	7.743	8.1109	9.9388	74.4956	79.973	63.5775	537.54
2	7.6419	8.1676	9.9166	73.6854	79.4962	63.418	530.08
4	7.6845	8.1722	9.9313	73.4742	79.3993	63.4401	533.64
6	6.786	8.6395	8.9465	86.529	67.636	87.577	484.07
7	6.8906	8.7423	8.9861	86.7625	67.6771	87.7892	499.86
9	6.8054	8.7798	8.9781	86.909	68.214	88.185	497.37

The spectra of compounds involving Hdmax show broad bands in the 3400–3100 cm^{-1} region, assignable to ν(OH) of water, broadened and lower wavenumber displaced by the hydrogen bonds. The free ligand also displays a broad absorption around 2800 cm^{-1}, which disappears in the sodium salt and in the complexes, probably related with the acidic proton of the imidazole ring, extensively associated in H-bonding. For H3max compounds, the region where ν(OH) bands appear is wider (3500–3000 cm^{-1}), with a higher number of better defined bands. An additional intense and well-defined band appears at 2855 (free ligand), 2816 (Na salt) or 2840 cm^{-1} (complexes), that we assign to ν(N6–H), well defined but considerably displaced to lower wavenumbers due to the formation of the above mentioned DA–AD H-bond motif. The metal complexes also present wide absorptions in the 400–600 cm^{-1} region, attributable to rocking frequencies of water.

The first step of the thermal decomposition of the isolated complexes, as shown by their TG and DSC diagrams, is their dehydration. All compounds except **3** and **8** display a well-defined weight loss effect in the range 70–152 °C which agree well with the elimination of the water molecules indicated by their elemental analysis. Dehydration takes place in a single step (endothermic peaks in the range 100–140 °C) except for **1** for which two well-defined stages are observed (peaks at 105 and 140 °C). Dehydration energy is very similar for all compounds, ranging from 44.2 to 51.3 *kJ/mol* of water. For **3** and **8**, the experimental values for weight losses are lower than the theoretical and dehydration enthalpies cannot be reliably obtained from the integration of the peaks in the DSC diagrams, suggesting that dehydration partially occurs at room temperature. Dehydrated complexes are stable in an wide temperature range (up to 300 °C for Mn(II), Co(II) and Ni(II), 330 °C for Zn(II) and Cd(II)-3max complexes and 400 °C for Zn(II) and Cd(II)-dmax complexes). In most cases, and previously to pyrolytic decomposition, a small exothermic peak appears that suggests an structural change before the pyrolysis of the organic moiety. Decomposition processes normally occurs in one step (300–500 °C for Mn(II), Co(II) and Ni(II)) or several steps (330–700 °C for Zn(II) and Cd(II)-3max complexes and 400–700 °C for Zn(II) and Cd(II)-dmax complexes), giving the corresponding metal oxide as residue.

The diffuse reflectance spectra of **2**, **3**, **7** and **8** are typical of octahedral species [30]. Cobalt compounds exhibit two main absorptions: a very broad one centred around 8500 cm^{-1}, assigned to the $^4T_{2g}(F) \leftarrow {}^4T_{1g}(F)$ (ν_1) transition and another one at 20790 (**2**) and 21834 (**7**) cm^{-1} assigned to the $^4T_{1g}(P) \leftarrow {}^4T_{1g}(F)$ (ν_3)transition. The lack of precision in the reading of the first band do not let us to perform a calculation of the ligand field parameters. The spectra for nickel compounds show two of the three typical bands expected for octahedral Ni(II) complexes at 10471 ($^3T_{2g}$ $(F) \leftarrow {}^3A_{2g}(F)$, ν_1) and 17361 ($^3T_{1g}$ $(F) \leftarrow {}^3A_{2g}(F)$, ν_2) cm^{-1} for **3** and 10417 and 17007 cm^{-1} for **8**, from which the parameters Δ_o = 10471 cm^{-1} and B = 1106 cm^{-1} for **3** and Δ_o = 10417 cm^{-1} and B = 964 cm^{-1} for **8** were calculated using Dou equations [31]. These values are closer to those of cromophores with N atoms involved in the coordination sphere than to that of the $[Ni(H_2O)_6]^{2+}$ cation [30], suggesting that there is a direct bond between the metal and the heterocycle for the nickel compounds.

We have measured ^1H and ^{13}C NMR spectra for the ligands, their sodium salts and the Zn(II) and Cd(II) complexes in dmso-d_6 (see the data in the experimental section). The spectra for the compounds with the same ligand are virtually identical, without any signal assignable to N2-H, indicating that the free ligands are mostly dissociated at the working concentration and that there is little or no interaction between ligands and metals in dmso solution.

4 Supplementary material

CCDC 687074, 687075 and 687076 contain the supplementary crystallographic data for this paper. These data can be obtained free of charge from The Cambridge Crystallographic Data Centre via www.ccdc.cam.ac.uk/data_request/cif.

Acknowledgements

This work was supported by a project of the Ministry of Education and Science of Spain (Project: CTQ-2005-00329/BQU) and the Junta de Andalucía (FQM00425). C.R. Maldonado is grateful for a FPU Grant from the Ministry of Education and Science of Spain.

References

[1] S.A. Kazakov, S.M. Hecht, Nucleic Acid–Metal Ion Interactions, Encyclopedia of Inorganic Chemistry, John Wiley & Sons, 2006.
[2] L.J. Prins, D.N. Reinhoudt, P. Timmerman, Angew. Chem., Int. Ed. 40 (2001) 2382.
[3] T. Steiner, Angew. Chem. Int. Ed. 41 (2002) 48.
[4] A.D. Burrows, Struct. Bond. 108 (2004) 55.
[5] H.U. Lanki, I. Wempen, J.J. Fox, J. Org. Chem. 35 (1970) 1131.
[6] M.P. Sánchez, M.A. Romero, J.M. Salas, D.J. Cárdenas, J. Molina, M. Quirós, J. Mol. Struct. 344 (1995) 257.
[7] C.R. Maldonado, M. Quirós, J.M. Salas, Acta Crystallogr., Sect. C 62 (2006) o–489.
[8] A. Holý, H. Dvořáková, J. Jindřich, M. Masojídková, M. Buděšínský, J. Balzarini, G. Andrei, E.D. Clercq, J. Med. Chem. 39 (1996) 4073.
[9] I. Giorgi, A.M. Bianucci, G. Biagi, O. Livi, V. Scartoni, M. Leonardi, D. Pietra, A. Coi, I. Massarelli, F.A. Nofal, F.L. Fiamingo, P. Anastasi, G. Giannini, Eur. J. Med. Chem. 42 (2007) 1.
[10] L.G. Purnell, J.C. Shepherd, D.J. Hodgson, J. Am. Chem. Soc. 97 (1975) 2376.
[11] L.G. Purnell, D.J. Hodgson, Biochim. Biophys. Acta 447 (1976) 117.
[12] L.G. Purnell, E.D. Estes, D.J. Hodgson, J. Am. Chem. Soc. 98:3 (1976) 740.
[13] L.G. Purnell, D.J. Hodgson, J. Am. Chem. Soc. 99:11 (1977) 3651.
[14] B.J. Graves, D.J. Hodgson, Inorg. Chem. 20 (1981) 2223.
[15] N. Katsaros, A. Grigoratos, Inorg. Chim. Acta 108 (1985) 173.
[16] E. Colacio, M.A. Romero, M. Nogueras, A. Sánchez, J.L. Estrella, An. Quím. (1986) 240.
[17] V. Ravichandran, G.A. Ruban, K.K. Chacko, M.A. Romero, E. Colacio, J.M. Salas, K. Aoki, H. Yamazaki, J. Chem. Soc., Chem. Commun. (1986) 1780.
[18] W.S. Sheldrick, P. Bell, Inorg. Chim. Acta 123 (1986) 181.
[19] W.S. Sheldrick, P. Bell, Z. Naturforsch. B 41 (1986) 1117.
[20] W.S. Sheldrick, P. Bell, Z. Naturforsch. B 42 (1987) 195.
[21] W.S. Sheldrick, B. Günther, Inorg. Chim. Acta 152 (1988) 223.
[22] W.S. Sheldrick, P. Bell, Inorg. Chim. Acta 160 (1989) 265.
[23] W.S. Sheldrick, B. Günther, J. Organomet. Chem. 375 (1989) 233.
[24] W.S. Sheldrick, G. Heeb, Inorg. Chim. Acta 190 (1991) 241.
[25] G. Nübel, W. Pfleiderer, Chem. Ber. 98 (1965) 1060.
[26] G.M. Sheldrick, SHELXL-97, University of Göttingen, Germany, 1997.
[27] Bruker AXS, TOPAS-R: General profile and structure analysis software for powder diffraction data.
[28] M.C. Etter, J. Phys. Chem. 95 (1991) 4601.
[29] J. Bernstein, R.E. Davis, L. Shimoni, N.-L. Chang, Angew. Chem., Int. Ed. Engl. 34 (1995) 1555.
[30] A.B.P. Lever, Inorganic Electronic Spectroscopy, Elsiever, Amsterdam, 1986.
[31] Y. Dou, J. Chem. Ed. 67 (1990) 134.